

THE RESPONSE MATRIX ACCELERATION METHOD FOR THE DISCRETE-ORDINATE TRANSPORT EQUATION

Wesley Ford¹, Emiliano Masiello¹,

Christophe Calvin¹, François Fevotte², Bruno Lathuilliere²

¹DEN-Service d'études des réacteurs et de mathématiques appliquées (SERMA),
CEA, Université Paris-Saclay, F-91191, Gif-sur-Yvette, France

²Electricite de France
91120 Palaiseau, France

wesley.ford@cea.fr, emiliano.masiello@cea.fr,
christophe.calvin@cea.fr, francois.fevotte@edf.fr, bruno.lathuilliere@edf.fr

ABSTRACT

In this paper, we propose a new non-linear technique for accelerating the source iterations of the discrete ordinates transport equation. The new method, called Response Matrix Acceleration (RMA), has been designed to complement the Coarse-Mesh Finite Difference method (CMFD) by offering better stability and improved performance in cases where CMFD fails. To accomplish this, RMA uses knowledge of the transport operator along with nonlinear coefficients and solves for the interface partial currents to maintain consistency with the transport operator. Two distinct variants of RMA are derived. The convergence properties of both variants of RMA applied to two distinct iteration schemes of the step short method of characteristics (MOSC) transport operator are investigated. The results of a spectral radius analysis are presented, along with a numerical benchmark of the ZPPR and the C5G7 problems in 3D. Analysis of the results indicates that both variants of RMA have improved effectiveness and stability relative to CMFD, for optically diffusive materials. To achieve optimal numerical performance, a combination of RMA and CMFD is suggested. Improvements in the performance of RMA are expected with ongoing development and optimization. Further investigation into the use of RMA for accelerating outer iterations, parallel problems, and different transport operators is proposed.

KEYWORDS: Discrete-ordinates transport equation, non-linear acceleration, stability analysis, Spectral radius analysis, CMFD

1. INTRODUCTION

The time to solution of large-scale deterministic neutron transport codes are often based on the synergy of the source iteration operator (SI operator, also referred here as the transport operator) and the acceleration operator. While the transport operator defines the accuracy of the results, the acceleration operator speeds up the convergence of SI. This acceleration is typically achieved by converging the scattering and fission source. The SI operator alone converges in a reasonable

time only when the problem is dominated by absorption and high rates of leakage. Contrarily, for the simulation of a nuclear reactor, SI shows poor performances since the transport regime is dominated by scattering [1].

One of the most prevalent acceleration methods, the Coarse Mesh Finite Difference method (CMFD), has proven to be effective especially in synergy with the step short method of characteristics (MOSC) [2]. The non-linear nature of the acceleration has allowed it to effectively reduce the number of transport iterations while reducing the memory footprint. However, CMFD can lead to unstable or divergent iteration behavior for some critical spatial configurations. Cho and Park have shown that CMFD is effective when the coarse cell optical thickness does not exceed 1 mean free path (mfp), but becomes rapidly unstable for cells with large optical thicknesses [3].

In this article we propose a new nonlinear DP0 method, called the Response Matrix Acceleration method (RMA), which is meant to address the flaws of CMFD. RMA has been designed to complement CMFD by offering better stability and improved performance in cases where CMFD is ineffective. To achieve this, RMA uses knowledge of the transport operator along with nonlinear coefficients to maintain consistency with the transport operator. As well, RMA solves for the interface partial currents, to increase its degrees of freedom relative to CMFD, while being able to scale for multidimensional and, especially for unstructured meshes. Due to its three dimensional implementation of MOSC and its prominence, the code IDT, developed as a solver for APOLLO3 by the Laboratoire de Transport Stochastique et Deterministe (LTSD) at CEA Saclay, was chosen as the neutron transport solver.

This article has been organized into two parts. First we will derive RMA, and state the transport iteration schemes that we will be analyzing. Next, we will display and discuss the results of a spectral radius analysis and a numerical benchmark of RMA and the MCNH variant of CMFD [2].

2. RESPONSE MATRIX ACCELERATION

It is important to note that while during this derivation RMA will only be applied to MOSC, although RMA is capable of being applied to any conservative transport operator due to its nonlinearity. For simplicity, during this derivation the transport operator and RMA share the same spatial mesh, though results for homogenized pin cells are presented later for the 3D C5G7. For clarity, all nonlinear terms are accented with a tilde. We begin our derivation of RMA with the step MOSC equations for a problem with a fixed external source [4],

$$\psi_{m,i,s}^+ = \sum_{s' \in S_{m,i,s}} T_{m,i,s,s'} \psi_{m,i,s'}^- + E_{m,i,s} Q_{m,i}, \quad (1a)$$

$$\bar{\phi}_{l,k,i} = \sum_{m=1}^M w_m Y_{l,k}(\hat{\Omega}_m) \sum_{s \in S_i} I_{m,i,s} \psi_{m,i,s}^- + C_{m,i} Q_{m,i}, \quad (1b)$$

$$Q_{m,i} = \sum_{l=0}^L \sum_{k=-l}^l Y_{l,k}(\hat{\Omega}_m) [\Sigma_{s,l,i} \bar{\phi}_{l,k,i} + q_{l,k,i}]. \quad (1c)$$

- m, i, s , are the angular direction, spatial cell, and cell surface indices respectively.
- $S_{m,i,s}$, is the set of surfaces of cell i that contribute to surface s along direction m .

- $T_{m,i,s,s'}$, $E_{m,i,s}$, $I_{m,i,s}$ and $C_{m,i}$, are the MOSC coefficients that define the transmission of the uncollided flux from surface s' to surface s , the escape of the collided flux to surface s , the contribution of the incident uncollided flux to the average flux, and the contribution of the collided flux to the average flux respectively.
- $\psi_{m,i,s'}^-$ and $\psi_{m,i,s}^+$, are the incoming and outgoing angular flux respectively.
- w_m and $\hat{\Omega}_m$, are the weight of the angular quadrature and the angular direction respectively.
- $\bar{\phi}_{l,k,i}$ and $Q_{m,i}$, are the angular moment of the cell averaged flux for degree l and order k , and the fixed source respectively.
- $Y_{l,k}$ and $\Sigma_{s,l,i}$, are the real spherical harmonic function [5] and the angular moment of the scattering cross section respectively.

In order to solve for the interface partial currents, we assume that the relative surface angular flux distribution is fixed within each angular hemisphere, such that

$$\psi_{m,i,s}^\pm = \tilde{h}_{m,i,s}^\pm J_{i,s}^\pm, \quad (2a)$$

$$J_{i,s}^\pm = \sum_{m \in M_s^\pm} \left| w_m \hat{\Omega}_m \cdot \hat{n}_s \right| \psi_{m,i,s}^\pm. \quad (2b)$$

Where $J_{i,s}^-$ and $J_{i,s}^+$ are the incoming and outgoing partial currents. \hat{n}_s is the unitary vector that defines the normal of surface s pointing outward from the cell. $\tilde{h}_{m,i,s}^-/+$ is the nonlinear coefficient set such that Eq. (2a) is satisfied. Finally, M_s^\pm are the set of outgoing and incoming directions that intersect surface s . Substituting Eq. (2a) into Eq. (1a) gives us,

$$\tilde{h}_{m,i,s}^+ J_{i,s}^+ = \sum_{s' \in S_{m,i,s}} T_{m,i,s,s'} \tilde{h}_{m,i,s'}^- J_{i,s'}^- + E_{m,i,s} Q_{m,i}. \quad (3)$$

Expanding $Q_{m,i}$ in terms of $Y_{l,k}(\hat{\Omega}_m)$ outside of , and summing Eq. (3) over $m \in M_s^+$ gives us,

$$\begin{aligned} \sum_{m \in M_s^+} w_m \tilde{h}_{m,i,s}^+ J_{i,s}^+ &= \sum_{m \in M_s^+} w_m \sum_{s' \in S_{m,i,s}} T_{m,i,s,s'} \tilde{h}_{m,i,s'}^- J_{i,s'}^- \\ &+ \sum_{l=0}^L \sum_{k=-l}^l \sum_{m \in M_s^+} Y_{l,k}(\hat{\Omega}_m) w_m E_{m,i,s} Q_{l,k,i}. \end{aligned} \quad (4)$$

We simplify the notation by introducing the nonlinear variables $\tilde{T}_{i,s,s'}$ and $\tilde{E}_{l,k,i,s}$,

$$J_{i,s}^+ = \sum_{s' \in S_{i,s}} \tilde{T}_{i,s,s'} J_{i,s'}^- + \sum_{l=0}^L \sum_{k=-l}^l \tilde{E}_{l,k,i,s} Q_{l,k,i}, \quad (5a)$$

$$\tilde{T}_{i,s,s'} = \frac{\sum_{m \in M_s^+ \cap M_{s'}^-} w_m \tilde{h}_{m,i,s'}^-}{\sum_{m \in M_s^+} w_m \tilde{h}_{m,i,s}^+}, \quad (5b)$$

$$\tilde{E}_{l,k,i,s} = \frac{\sum_{m \in M_s^+} Y_{l,k}(\hat{\Omega}_m) w_m E_{m,i,s}}{\sum_{m \in M_s^+} w_m \tilde{h}_{m,i,s}^+}. \quad (5c)$$

Where $S_{i,s}$ is the set of surfaces of cell i whose incoming angular flux contributes to the outgoing angular flux of surface s . The next step towards forming a closed system of equations is to rewrite

$Q_{l,k,i}$ in terms of the partial currents. First, we define the nonlinear relation,

$$\tilde{E}_{i,s} = \sum_{l=0}^L \sum_{k=-l}^l \tilde{E}_{l,k,i,s} Q_{l,k,i} / Q_{0,0,i}. \quad (6)$$

It is important to note that Eq. (6), takes into account the anisotropy of the source. Substituting Eq. (6) and the definition of the source from Eq. (1b), into Eq. (5a) gives us,

$$J_{i,s}^+ = \sum_{s' \in S_{i,s}} \tilde{T}_{i,s,s'} J_{i,s'}^- + \tilde{E}_{i,s} [\Sigma_{s,0,i} \bar{\phi}_{0,0,i} + q_{0,0,i}]. \quad (7)$$

The next step is to define the relationship between the partial current and $\bar{\phi}_{0,0,i}$. There are two distinct approaches for accomplishing this that will lead us to the Explicit RMA (E-RMA) and Balance RMA (B-RMA) variants of the RMA method.

2.1. Closure relation for explicit RMA

We start from the step MOSC relation for the average scalar flux, as defined by Eq. (1c),

$$\bar{\phi}_{0,0,i} = \sum_{m=1}^M w_m \sum_{s \in S_i} I_{m,i,s} \psi_{m,i,s}^- + C_{m,i} Q_{m,i}. \quad (8)$$

Again, expanding $Q_{m,i}$ in terms of $Y_{l,k}(\hat{\Omega}_m)$, and substituting Eq. (2a) in to the above equation gives us,

$$\bar{\phi}_{0,0,i} = \sum_{s \in S_i} \tilde{I}_{i,s} J_{i,s}^- + \sum_{l=0}^L \sum_{k=-l}^l \tilde{C}_{l,k,i} Q_{l,k,i}, \quad (9a)$$

$$\tilde{I}_{i,s} = \sum_{m \in M_s^-} w_m \frac{I_{m,i,s} \psi_{m,i,s}^-}{J_{i,s}^-}, \quad (9b)$$

$$\tilde{C}_{l,k,i} = \sum_{m=1}^{M^-} w_m Y_{l,k}(\hat{\Omega}_m) C_{m,i}. \quad (9c)$$

Where S_i is the set of all the surfaces of cell i . Next, we define the nonlinear relation,

$$\tilde{C}_i = \sum_{l=0}^L \sum_{k=-l}^l \tilde{C}_{l,k,i} Q_{l,k,i} / Q_{0,0,i}. \quad (10)$$

and substitute it, along with the definition of the source from Eq. (1b), into Eq. (9a) to get,

$$\bar{\phi}_{0,0,i} = \sum_{s' \in S_i} \tilde{I}_{i,s} J_{i,s'}^- + \tilde{C}_i [\Sigma_{s,0,i} \bar{\phi}_{0,0,i} + q_{0,0,i}]. \quad (11)$$

Finally we combine like terms and solve $\bar{\phi}_{0,0,i}$ to be,

$$\bar{\phi}_{0,0,i} = \sum_{s \in S_i} \frac{\tilde{I}_{i,s}}{1 - \Sigma_{s,0,i} \tilde{C}_i} J_{i,s}^- + \frac{\tilde{C}_i}{1 - \Sigma_{s,0,i} \tilde{C}_i} q_{0,0,i}, \quad (12)$$

which specifies the E-RMA.

2.2. Closure relation for balance RMA

The second approach is based on the balance equation in terms of the scalar flux,

$$\bar{\phi}_{0,0,i} = \frac{\sum_{s \in S_i} A_{i,s} [J_{i,s}^- - J_{i,s}^+] + q_{0,0,i} V_i}{[\Sigma_i - \Sigma_{s,0,i}] V_i}. \quad (13)$$

Where Σ_i, V_i and $A_{i,s}$ are the total cross section, the volume of cell i , and the surface area of surface s of cell i , respectively. This approach is attractive since it requires the computation of less nonlinear coefficients, and it is simpler to implement than the previous approach. However the scalar flux is now dependent on both the incoming and outgoing partial currents, which would result in a matrix with twice the coupling of that produced by the previous approach.

2.3. Solving RMA

By substituting in either of the above closure relations into Eq. (7), applying the transport boundary conditions, and by enforcing continuity at the interfaces, we get a system of equations of the form,

$$J^+ = \tilde{A} J^+ + Q_{Ac}. \quad (14)$$

Where J^+ is the acceleration solution vector, which is comprised of the outgoing partial current. Ψ is the transport solution vector. \tilde{A} is the nonlinear operator formed from the terms of Eq. (7) that contain the partial current. Finally, Q_{Ac} is the acceleration source, which is made up of the constant terms of Eq. (7) and the external boundary source. To solve Eq.(14), we use the bi-stabilized conjugate gradient method [6] and the following iteration scheme,

$$\left[I - \tilde{A}^{(n+1/2)} \right] J^{+, (n+1)} = Q_{Ac}^{(n+1/2)}, \quad (15)$$

where n is the iteration index. After Eq. (15) has been solved, $\psi_{m,i,s}^-, \psi_{m,i,s}^+$ are corrected according to Eq. (2a),

$$\psi_{m,i,s}^{\pm, (n+1)} = \tilde{h}_{m,i,s}^{\pm, (n+1/2)} J_{i,s}^{\pm, (n+1)}, \quad \text{when } \left| \hat{\Omega}_m \cdot \hat{n}_s \right| < 0. \quad (16)$$

Instead, the $\bar{\phi}_{l,k,i}$ is updated by the rebalancing relation,

$$\bar{\phi}_{l,k,i}^{(n+1)} = \bar{\phi}_{l,k,i}^{(n+1/2)} \frac{\bar{\phi}_{0,0,i}^{(n+1)}}{\bar{\phi}_{0,0,i}^{(n+1/2)}}. \quad (17)$$

3. ITERATION SCHEMES

This work is a preliminary investigation for accelerating parallel transport simulation by non-linear schemes. Even though we do not present numerical results for parallel simulations, we are still interested in investigating the convergence of RMA for spatially decomposed problems. The iteration

scheme in this case is

$$\psi_{m,i,s}^{+,(n+1/2)} = \sum_{s' \in S_{m,i,s}} T_{m,i,s,s'} \psi_{m,i,s'}^{-,(n)} + E_{m,i,s} Q_{m,i}^{(n)}, \quad (18a)$$

$$\bar{\phi}_{l,k,i}^{(n+1/2)} = \sum_{m=1}^M w_m Y_{l,k}(\hat{\Omega}_m) \left\{ \sum_{s \in S_i} I_{m,i,s} \psi_{m,i,s}^{-,(n)} + C_{m,i} Q_{m,i}^{(n)} \right\}, \quad (18b)$$

$$Q_{m,i}^{(n+1)} = \sum_{l=0}^L \sum_{k=-l}^l Y_{l,k}(\hat{\Omega}_m) \left[\sum_{s,l,i} \bar{\phi}_{l,k,i}^{(n+1)} + q_{l,k,i} \right], \quad (18c)$$

where all of the interface angular flux are simultaneously updated each iteration. We will refer to this scheme as a Gauss-Jacobi scheme. The second scheme is the standard transport sweeping,

$$\psi_{m,i,s}^{+,(n+1/2)} = \sum_{s' \in S_{m,i,s}} T_{m,i,s,s'} \psi_{m,i,s'}^{-,(n+1/2)} + E_{m,i,s} Q_{m,i}^{(n)}, \quad (19a)$$

$$\bar{\phi}_{l,k,i}^{(n+1/2)} = \sum_{m=1}^M w_m Y_{l,k}(\hat{\Omega}_m) \left\{ \sum_{s \in S_i} I_{m,i,s} \psi_{m,i,s}^{-,(n+1/2)} + C_{m,i} Q_{m,i}^{(n)} \right\}, \quad (19b)$$

$$Q_{m,i}^{(n+1)} = \sum_{l=0}^L \sum_{k=-l}^l Y_{l,k}(\hat{\Omega}_m) \left[\sum_{s,l,i} \bar{\phi}_{l,k,i}^{(n+1)} + q_{l,k,i} \right], \quad (19c)$$

where each interface incoming angular flux is updated by the upstream interface angular flux from the previous region. By comparing the two schemes, they are distinguished by the iteration index of the interface angular flux that appears on the right hand side of the system of equations. It is important to note that for either iteration scheme the incoming boundary angular flux are from the previous iteration. Thus, at very low optical thicknesses, the spectral radius is dominated by the anisotropic eigenvalue corresponding to the transmission of the unconverged incoming angular flux, [7]. This can be easily seen in the case when we have a beam transversing a slab, with $\tau \rightarrow \epsilon$. By applying either Eqs. (19a) to (19c) or Eqs. (18a) to (18c) to this case we can see that the outgoing angular flux depends on the incoming boundary angular flux by the following relation.

$$\psi_{m,i,s}^{+,(n+1/2)} = \sum_{s' \in S_{m,i,s}} T_{m,i,s,s'} \psi_{m,i,s'}^{-,(n)} + o(\epsilon),$$

$$T_{m,i,s,s'} = \int_{\Gamma_s \cap \Gamma_{s'}} ds' \left| \hat{\Omega} \cdot \hat{n}_{s'} \right| e^{-\Sigma_i l_{m,i}(s)}.$$

Where, $l_{m,i}(s)$ is the chord length between surface s' and surface s , along direction m , and $c_{l,i}$ is the scattering ratio. We can easily see that the spectral radius of the above relation is the exponential term. A good source of reference on this topic is [7], since it contains a detailed analysis of the convergence behavior for this type of transport iteration scheme.

4. RESULTS OF SPECTRAL RADIUS ANALYSIS

The effectiveness of RMA and of CMFD when applied to the source iteration of the step MOSC has been investigated with a spectral radius analysis applied to 1D geometry infinite homogeneous medium. A S_8 angular distribution is used to represent the angular flux. The test analyzes the

influence of the optical thickness and the scattering ratio on the spectral radius. Both transport iteration schemes are investigated, the Gauss-Jacobi and the standard transport sweep. The results of this analysis are shown in Fig. 1. It is remarkable, that the spectral radius of both versions of RMA are significantly reduced compared to CMFD for optically diffusive mediums. Furthermore, both RMA are stable throughout the domain, unlike CMFD when τ is greater than 1 mfp. Both RMA methods and CMFD are effective when $\tau \in [0.1, 1]$, as predicted in [3] for the CMFD. For all operators, the Gauss-Jacobi iteration scheme has a higher spectral radius than that of the equivalent standard iteration scheme. This indicates that RMA will be effective for parallel acceleration. However, both RMA methods are still effective for the Gauss-Jacobi interface angular flux update.

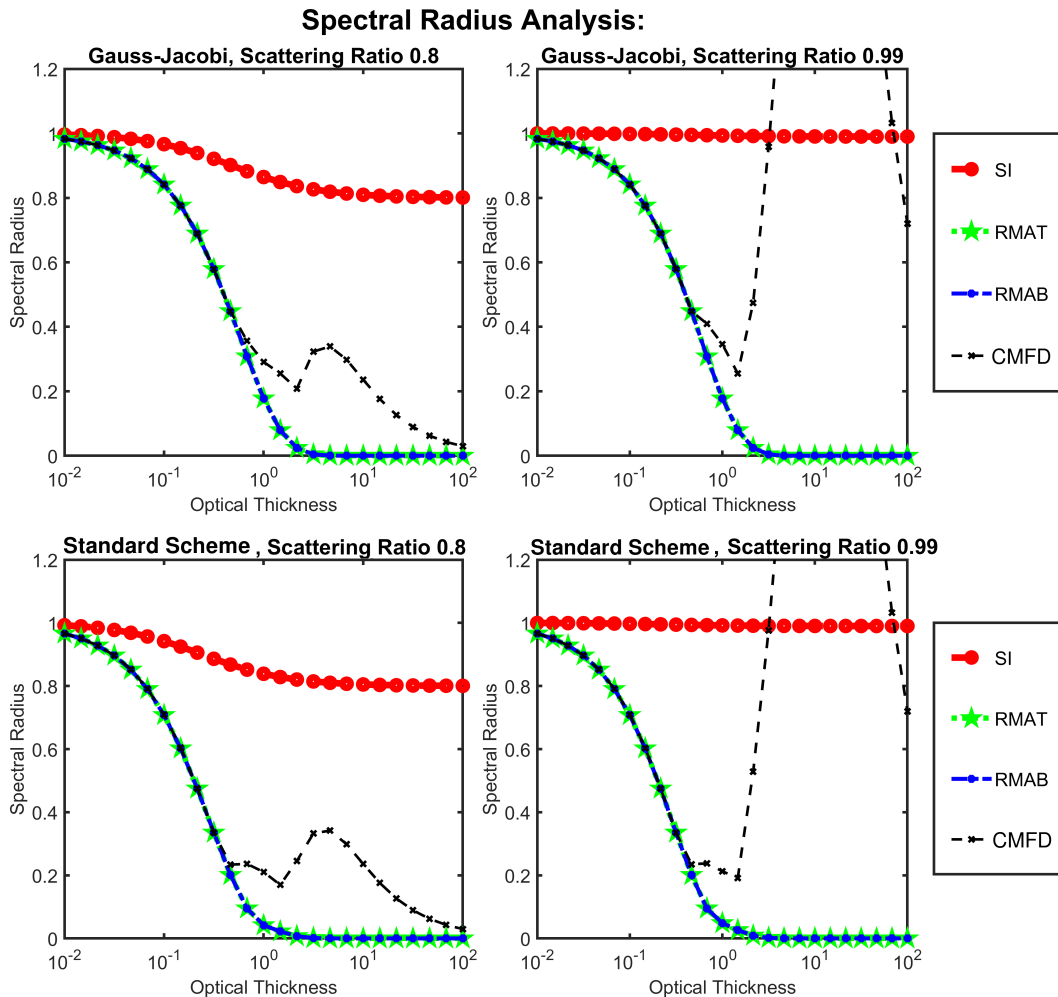


Figure 1: Displays the spectral radius of both variants of RMA, CMFD, and SI for the previously defined problem.

5. RESULTS OF NUMERICAL BENCHMARK

For this test suite, we focus only on the acceleration of the inner iterations. For all the cases presented, the inner iterations are fully converged per each outer iteration. Also, each simulation has been run on a single thread. For all cases, a S16 angular distribution is used to discretize the

angular domain, and the step MOSC is used for the spatial domain. The first benchmark is the 3D model of the Zero Power Physics Reactor (ZPPR) [8], P0-corrected 16-group cross section library. The results of this benchmark are shown below in Tables 1 and 2. As shown in Table 1, CMFD is unstable without converging. On the other hand, both variants of RMA reduce the number of inner iterations by a factor of 22. However, the runtime for both methods is longer than that of transport alone. As explained by Table 2, this is because the code responsible for the generation of the operators is under development, with a focus on generality and transparency rather than optimization. This lack of optimization will be addressed in future but our current goal is the reduction of inner iterations. In contrast, the inversion of the acceleration operator takes up only a few percent of the total elapsed time.

Table 1: Contains the results of ZPPR benchmark

Acceleration Type	# of Outer Iter.	# of Inner Iter.	Runtime (h)	Speedup in Time	Speedup in Iter.
SI	114	40197	50.3	1.00	1.00
CMFD	NC	NC	NC	NC	NC
E-RMA	105	1822	65.0	0.774	22.1
B-RMA	105	1822	59.2	0.850	22.1

Table 2: Contains the profiling data of the acceleration operators for the ZPPR benchmark

Acceleration Type	Time to Solve Operator (h)	Time to Solve Operator (%)	Time to Generate Operator (h)	Time to Generate Operator (%)
E-RMA	2.48	3.82	62.8	92.7
B-RMA	3.64	6.15	56.9	89.9

The next test is the 3D rodded-B configuration of the C5G7 MOX benchmark [9]. The results of this benchmark are shown below in Tables 3 and 4. Unlike the ZPPR, the mesh of RMA is homogenized at the pin cell level. Because of the homogenization, there is a large reduction in the cost of computing RMA relative to the transport.

Based off the results of the spectral radius analysis, we concluded that we could optimize the ratio between the computational cost of the acceleration and its effectiveness, by using RMA when $\tau > 1$ and CMFD otherwise. We will refer to the resulting combination of the two methods as the hybrid method. As Table 3 shows, the best speedup in time and number of iterations is achieved by the hybrid method. Both variants of RMA reduce the number of iterations more effectively than CMFD, but are less effective at reducing the time. As previously discussed, and as evidenced by

Table 4, this difference between speedups is due to the lack of optimization of the code responsible for the generation of the operator. We can also observe that the computational overhead for solving the RMA operator relative to CMFD is roughly proportional to the number of surfaces. However, since the inversion of the acceleration operator makes up only a few percentages of the overall simulation time, the extra computational incurred by RMA is almost inconsequential.

Table 3: Contains the results of C5G7 benchmark

Acceleration Type	# of Outer Iter.	# of Inner Iter.	Runtime (h)	Speedup in Time	Speedup in Iter.
SI	51	8352	70.0	1.00	1.00
CMFD	51	3302	29.2	2.40	2.53
E-RMA	51	3018	53.9	1.30	2.77
B-RMA	51	2993	49.2	1.42	2.79
Hybrid	51	1788	18.6	3.76	4.67

Table 4: Contains the profiling data of the acceleration operators for the C5G7 benchmark

Acceleration Type	Time to Solve Operator (h)	Time to Solve Operator (%)	Time to Generate Operator (h)	Time to Generate Operator (%)
CMFD	1.23×10^{-1}	0.424	1.37	4.69
E-RMA	6.19×10^{-1}	1.14	28.1	51.9
B-RMA	7.69×10^{-1}	1.56	24.3	49.5
Hybrid	1.45×10^{-1}	0.779	3.47	18.7

6. CONCLUSIONS

In this article, we propose a new acceleration method called the Response Matrix Acceleration method (RMA). RMA improves upon the effectiveness and the stability of CMFD for optically diffusive geometries. In fact, RMA has been shown to be stable for all the cases studied. This result has been verified by means of spectral radius analysis and numerical benchmarks. For optically thin medium, RMA and CMFD are equivalently effective, making CMFD the better choice in this regime due to its lower cost. Which leads us to conclude that a combination of CMFD with RMA leads to the best numerical performance.

For all the cases studied, the same spatial mesh was used for the transport and the acceleration operators. Further investigation will be done by applying the RMA operator to coarse meshes. This

field will be important to find the compromise between the numerical efficiency and the effectiveness of the acceleration. We have also limited the application of RMA to the inner iterations, but we are currently working towards using RMA for accelerating the power and thermal iterations. Finally the investigation of RMA for spatially decomposed problems is currently underway.

ACKNOWLEDGEMENTS

This work has been jointly funded by Commissariat a l'Energie Atomique (CEA) and Electricite de France (EDF).

REFERENCES

- [1] M. L. Adams and E. W. Larsen. "Fast iterative methods for discrete-ordinates particle transport calculations." *Progress in Nuclear Energy*, **volume 40**(1), pp. 3–159 (2002).
- [2] H. T. Kim and Y. Kim. "Convergence Studies on Nonlinear Coarse-Mesh Finite Difference Accelerations for Neutron Transport Analysis." *Nuclear Science and Engineering*, **volume 191**(2), pp. 136–149 (2018). URL <https://doi.org/10.1080/00295639.2018.1463747>.
- [3] N. Cho and C. Park. "A Comparison of Coarse Mesh Rebalance and Coarse Mesh Finite Difference Accelerations for the Neutron Transport Calculations." *Nuclear Mathematical and Computational Sciences: A Century in Review* (2003).
- [4] J. Askew. "A characteristics formulation of the neutron transport equation in complicated geometries." *INIS* (1972).
- [5] E. Hobson. *The Theory of Spherical and Ellipsoidal Harmonics*. Chelsea Pub. Co. (1955).
- [6] Y. Saad. *Iterative Methods for Sparse Linear Systems*. University of Minnesota (2003).
- [7] R. Sanchez. "On the spectral analysis of iterative solutions of the discretized one-group transport equation." *Annals of Nuclear Energy*, **volume 31**, pp. 2059–2075 (2004).
- [8] L. G. LeSage. "AN OVERVIEW OF THE ARGONNE NATIONAL LABORATORY FAST CRITICAL EXPERIMENTS." Technical report, Argonne National Laboratory (2001). URL https://www.oecd-neo.org/science/wprs/irphe/irphe-handbook/documents/anl_nt_175.pdf.
- [9] B.-C. N. M.A. Smith, E. E. Lewis. "Benchmark on Deterministic Transport Calculations Without Spatial Homogenisation." Technical report, Nuclear Energy Agency (2003). URL <https://www.oecd-neo.org/science/docs/2003/nsc-doc2003-16.pdf>.